Available online at www.sciencedirect.com
SCIENCE DIRECT
Journal of Photochemistry and Photobiology A: Chemistry 176 (2005) 270–278
Journal of Photochemistry and Photobiology A:Chemistry
www.elsevier.com/locate/jphotochem

# Aircraft observations of daytime $NO_3$ and $N_2O_5$ and their implications for tropospheric chemistry

Steven S. Brown [a,b,*], Hans D. Osthoff [a,b], Harald Stark [a,b], William P. Dubé [a,b], Thomas B. Ryerson [a], Carsten Warneke [a,b], Joost A. de Gouw [a,b], Adam G. Wollny [a,b], David D. Parrish [a], Frederick C. Fehsenfeld [a], A.R. Ravishankara [a,c]

[a] *NOAA Aeronomy Laboratory, R/AL2, 325 Broadway, Boulder, CO 80305, USA*
[b] *Cooperative Institute for Research in the Environmental Sciences, University of Colorado, Boulder, CO 80309, USA*
[c] *Department of Chemistry and Biochemistry, University of Colorado, Boulder, CO 80309, USA*

**Abstract**

The nitrate radical ($NO_3$) and dinitrogen pentoxide ($N_2O_5$) are normally considered only in the context of nighttime atmospheric chemistry. Although their importance during the day is often small, it is not always negligible. Here, we present daylight observations of both compounds from the NOAA P-3 aircraft taken during the New England Air Quality Study in the summer of 2004. Observed mixing ratios agreed with predictions from a simple, rapidly established daytime steady state, although observed and calculated mixing ratios of $NO_3$ were near the instrumental detection limit. The observations have several implications for tropospheric chemistry during the daytime, including the loss of ozone through photolysis of $NO_3$ to $NO + O_2$, oxidation of biogenic volatile organic compounds (VOC), and conversion of $NO_x$ (=$NO + NO_2$) to $HNO_3$ via $N_2O_5$ hydrolysis. The magnitude of each process is considered in comparison to its photochemically driven analog. For example, $NO_3$ oxidation of α-pinene in the presence of $NO_x$ contributes 10–40% of the total daytime oxidation rate. Hydrolysis of $N_2O_5$ increases the daytime conversion rate of $NO_x$ to $HNO_3$ by several percent, with a maximum of 13%, relative to $OH + NO_2$. The implications of these observations for daytime $NO_3$ and $N_2O_5$ reactions in a variety of locations and seasons are discussed.


*Keywords:* Nitrate radical; Dinitrogen pentoxide

## 1. Introduction

The nitrate radical, $NO_3$, has been observed and shown to be an important oxidant during nighttime in the troposphere [1–6]. It is produced primarily from the reaction of $NO_2$ with ozone.

$$NO_2 + O_3 \rightarrow NO_3 + O_2 \quad (1)$$

Although there has been considerable study of the role of $NO_3$ in the dark, its importance to daytime atmospheric chemistry has been considered in detail only recently [7]. The lack of attention is for good reason; its daytime concentrations are normally quite small because $NO_3$ is efficiently photolyzed in sunlight and reacts rapidly with NO, which is a predominantly daytime species.

$$NO_3 + h\nu \rightarrow NO_2 + O \quad (2a)$$

$$NO_3 + h\nu \rightarrow NO + O_2 \quad (2b)$$

$$NO_3 + NO \rightarrow 2NO_2 \quad (3)$$

However, negligible concentrations do not mean negligible importance of the species in the atmosphere. A relatively large flux (from several hundred to several thousand pptv $h^{-1}$) of $NO_2$ oxidation by $O_3$ is required to support modest $NO_3$ and $N_2O_5$ concentrations during the day, and in the process, there can be significant impacts on $NO_x$, $O_3$ and volatile organic compounds (VOC).

The rate of $NO_3$ production via reaction (1) is not significantly altered between day and night, but its removal rate is increased drastically during daytime. However, under conditions of either strong source strength (i.e., large $NO_2$ and/or $O_3$) or weak sinks (e.g., reduced photolytic removal due to a decrease in solar flux under clouds), significant sustained concentrations of gas phase $NO_3$ during the day are possible. Geyer et al. [7] have delineated the conditions under which there can be several parts per trillion

* Corresponding author.

1010-6030/$ – see front matter © 2005 Elsevier B.V. All rights reserved.
doi:10.1016/j.jphotochem.2005.10.004

(pptv) mixing ratios of $NO_3$ in the daytime planetary boundary layer. Further, if the conditions are right, the removal of $NO_3$ by some processes can be comparable to or even larger than that via photolysis and reaction with NO. Examples include the scavenging of $NO_3$ into cloud droplets [8,9], ozone destruction in the stratosphere via the photolysis of $NO_3$ to give $NO + O_2$ [1], forest canopies where $NO_3$ could be a significant oxidizer for biogenic organics emitted there [10], and processing of $NO_x$ and $O_3$ in urban areas where the concentrations of both constituents are large enough to drive significant daytime $NO_3$ production [7].

Dinitrogen pentoxide, $N_2O_5$, forms from the addition of $NO_2$ to $NO_3$ and will also be present during the day in small concentrations under conditions favorable to the buildup of $NO_3$. Whereas removal processes for $NO_3$ must be competitive with its photolytic loss or NO reaction to be important during the day, removal processes for $N_2O_5$ that are competitive with its thermal dissociation to $NO_2 + NO_3$ will be of significance during the day. Hydrolysis of $N_2O_5$ is one of the primary pathways for conversion of $NO_x$ to nitric acid in the troposphere at night [11], but there is little information on the daylight role of $N_2O_5$ in the troposphere. As we will show below, however, this hydrolysis can enhance nitric acid production rates in sunlight.

This paper describes in situ measurements of $NO_3$ and $N_2O_5$ made in daylight from an aircraft using the high-sensitivity, direct absorption method of cavity-ring down spectroscopy (CaRDS). To our knowledge, this is the first report of direct measurements of $N_2O_5$ arising solely from a daytime source (i.e., not remaining from the previous night). We compare these observations to predictions based on a rapidly established steady state and discuss the implications of $NO_3$ and $N_2O_5$ in the presence of sunlight.

## 2. Field campaign and experiment

The New England Air Quality Study-Intercontinental Transport and Chemical Transformation (NEAQS-ITCT) field campaign in the summer of 2004 included deployments of several mobile platforms, including the NOAA WP-3D Orion aircraft, based out of Portsmouth, NH, and the NOAA research vessel (R/V) *Ronald H. Brown*, which sampled the outflow of the New England region in the Gulf of Maine. Each platform carried a suite of instruments for detailed characterization of gas phase composition, aerosol properties, radiation and meteorology. Of interest for the current analysis were measurements of $O_3$, NO and $NO_2$ via chemiluminescence [12], speciated volatile organic compounds by proton transfer reaction mass spectrometry (PTRMS) [13], aerosol number and size via optical particle counters [14] and speciated peroxy acetyl nitrates (PANs) by thermal dissociation chemical ionization mass spectrometry (TD-CIMS) [15].

The observations and analysis described here are unique because they combine daytime, in situ measurements of $NO_3$ and $N_2O_5$ via cavity ring-down spectroscopy [16] with direct measurements of the solar actinic fluxes that determine the rate of $NO_3$ photolysis, $j(NO_3)$, using spectral radiometers; this is a newly developed capability in our laboratory, and the details of the instrument and the reduction of the data to yield $j(NO_3)$ will be described in a forthcoming publication. The instrument retrieves actinic fluxes between 280 and 690 nm at 1 nm resolution using two separate spectrometers, and $NO_3$ photolysis rates were calculated from the measured solar fluxes using literature values for the $NO_3$ absorption cross section [17–19] and quantum yield [20,21]. The CaRDS instrument for $NO_3$ and $N_2O_5$ detection has been described in detail elsewhere [22–24]. It detects $NO_3$ optically on its strong visible absorption bands at 662 nm, and it detects the sum of $N_2O_5$ and $NO_3$ simultaneously on a second, heated channel that induces thermal decomposition of $N_2O_5$ to $NO_3$. Detection limits realized during NEAQS-ITCT were 0.4–1 pptv for $NO_3$ and 1–2 pptv for $N_2O_5$ ($2\sigma$, 1 s). As described below, this sensitivity is sufficient for frequent observation of $N_2O_5$ during the day, and for occasional observation of $NO_3$.

Measurements of $NO_3$ and $N_2O_5$ at levels near the instrumental detection limit during the day pose a particular challenge, and there are several potential limitations to the accuracy of the measurement. First, the instrument acquires a zero by titration of $NO_3$ with a small quantity (~25 ppbv) of NO added to the inlet, a procedure that is effective at night when there is little NO in the air, but that is less effective during the day when the small concentrations of $NO_3$ are already in steady state with the daytime levels of NO. In practice, this does not greatly affect the zeros since the added NO is well in excess of the concentrations normally present in the air, although for some large $NO_x$ plumes this effect can reduce the apparent $NO_3$ absorption signal. For measurement of $N_2O_5$, the NO present in the daytime air sample will partially titrate the $NO_3$ that comes from thermal conversion of $N_2O_5$ during the residence time required for this conversion in the heated inlet. We have made no attempt to correct the data for this effect, which should normally be small for most data reported here, but could result in as much as a 35% reduction in the $N_2O_5$ concentration. Therefore, values reported here for daytime $NO_3$ and $N_2O_5$ should be regarded as lower limits.

The most serious difficulty we encountered in the daytime measurements was a small 662 nm absorption signal in the heated channel that was uncorrelated with the predicted $N_2O_5$ concentrations but that was correlated with the mixing ratio of PAN ($CH_3C(O)O_2NO_2$) compounds. The origin of this signal is unclear. The sensitivity was variable, between 0 and 4 pptv of equivalent $N_2O_5$ signal per ppbv PAN, with a typical value less than 1 pptv $ppbv^{-1}$ when it was present. It could be an instrumental artifact arising from thermal dissociation of a PAN type compound followed by radical reactions in the heated inlet that generates an absorption at 662 nm. However, we are unaware of a chemical reaction scheme that would generate an absorbing species only in the absence of NO (e.g., schemes in which the NO reacts with the peroxy radicals generated from thermal dissociation of PAN should lead to a small, negative absorption signal due to the generation of $NO_2$ from the NO titrant during background acquisition). Furthermore, synthetic PAN samples introduced into the heated inlet in the laboratory yielded no measurable 662 nm absorption signal. The other possibility is a weak atmospheric source for $NO_3$ from chemical processes (e.g.,

photolysis, OH reactions, etc.) involving PAN or one of its speciated analogs. We are currently investigating both possibilities.

## 3. Calculated daytime steady states

Because photolytic destruction and NO reaction are rapid $NO_3$ sinks, the predicted daytime concentrations of $NO_3$ and $N_2O_5$ are quite small, at least for the summertime midlatitude conditions described here. These large sink terms also serve to establish a relatively rapid steady state in $NO_3$, so that its daytime concentration can be readily predicted. Consideration of reactions (1)–(3) alone gives a steady-state expression for the daytime $NO_3$ concentration.

$$[NO_3]_{Day} = \frac{k_1[O_3][NO_2]}{k_3[NO] + j_2} \quad (4)$$

Here, $k_1$ and $k_3$ are the bimolecular rate coefficients for reactions (1) and (3) and $j_2$ is the total first-order photolysis rate coefficient for $NO_3$ (i.e., the sum due to channels (2a) and (2b)). Under most daylight conditions, $NO_3$ photolysis and reaction with NO dominate over other losses such as $NO_3$ reactions with VOC or $N_2O_5$ hydrolysis. As noted by Geyer et al. [7] the $[NO_3]$ predicted by Eq. (4) becomes proportional to the square of the ozone concentration for large NO mixing ratios when the term $k_3[NO]$ dominates over $j_2$ (e.g., $k_3[NO] \approx 10 \times j_2$ for NO = 3 ppbv and clear skies). If $j_2$ is negligible, the ratio of $NO_2$ to NO can be substituted for the Leighton photostationary state expression [25].

$$NO + O_3 \rightarrow NO_2 + O_2 \quad (5)$$

$$NO_2 + h\nu + O_2 \rightarrow NO + O_3 \quad (6)$$

$$\frac{[NO_2]}{[NO]} = \frac{k_5[O_3]}{j_6} \quad (7)$$

$$[NO_3]_{Day} \approx \frac{k_1}{k_3}\frac{k_5}{j_6}[O_3]^2, \qquad k_3[NO] \gg j_2 \quad (8)$$

In the aircraft data presented here, the two terms in the denominator of Eq. (4) were often comparable; photolysis, rather than NO reaction, was frequently the larger pathway for $NO_3$ destruction, so that Eq. (4), rather than (8), was more appropriate. This is distinct from the cases observed by Geyer et al. [7] from surface measurements in Houston, TX, where daytime $NO_3$ formation was driven by large mixing ratios of $NO_x$ and $O_3$, and $NO_3$ reaction with NO was the dominant sink.

The concentration of $N_2O_5$ similarly follows a rapidly established steady state under warm conditions. This compound forms from its equilibrium with $NO_3$ and $NO_2$.

$$NO_3 + NO_2 \rightleftharpoons N_2O_5 \quad (9)$$

Assuming that rate coefficients for reactions consuming $N_2O_5$ (e.g., heterogeneous hydrolysis) are small in comparison to those for reactions that interconvert $NO_3$ and $N_2O_5$ (true for warm conditions where $k_{-9}$, the rate coefficient for the reverse of reaction (9) is rapid), the daytime concentration of $N_2O_5$ is given by:

$$[N_2O_5]_{Day} = K_{eq}[NO_2][NO_3]_{Day}. \quad (10)$$

Here, $K_{eq}$ is the equilibrium constant for reaction (9). Numerical modeling of the system including reactions (1)–(3), (9) validates the daytime steady-state expressions and shows that the approach to steady state requires less than 2 min for $T = 298$ K and $NO_2$ concentrations up to 10 ppbv. At 273 K, both steady-state expressions are still valid, but the time required for $N_2O_5$ to approach its steady state is approximately 1 h.

Reactions of $NO_3$ with VOCs are unlikely to significantly perturb the daytime steady-state concentrations predicted from these expressions. The lifetime of $NO_3$ with respect to VOC reactions is typically on the order of minutes, whereas its lifetime due to photolysis and/or reaction with NO is typically a few seconds or less. Hydrolysis of $N_2O_5$, on the other hand, can perturb these steady states, but only if it is rapid. Under warm conditions, even an $N_2O_5$ lifetime with respect to hydrolysis of 10 min, the fastest that we have observed, leads to a deviation from Eqs. (4) and (10) of <10% at 298 K. (As shown below, however, even a small perturbation to the $N_2O_5$ daytime steady state can be competitive with the reaction of OH with $NO_2$ as a daytime source for $HNO_3$.) The deviation from the steady-state expression for $N_2O_5$ can become larger at lower temperatures where the thermal dissociation rate coefficient for $N_2O_5$ becomes comparable to or even slower than its hydrolysis. For the data analyzed here under midlatitude summer conditions at low altitude, the steady-state expressions above are adequate.

## 4. Observed daytime abundances

Daytime $N_2O_5$ was observable on several occasions during NEAQS-ITCT 2004. Daytime $NO_3$, while observable, was typically at or near the instrumental detection limit.

As an example of the small size of the $NO_3$ signals, Fig. 1 shows a time series of one of the clearer comparison of measured

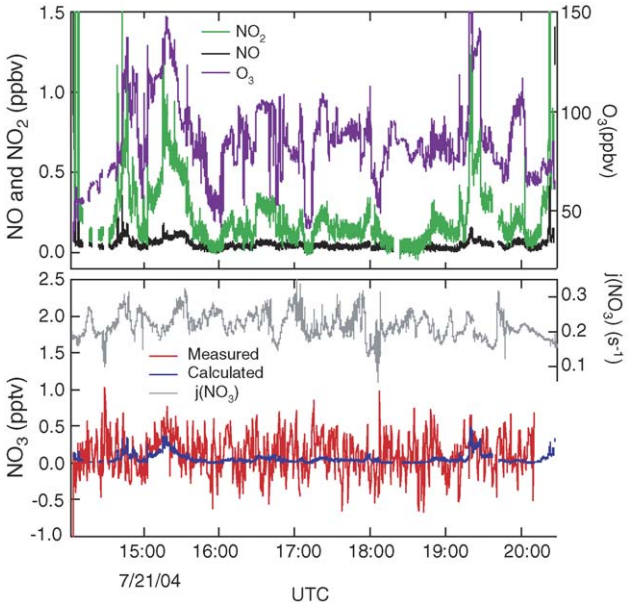


Fig. 1. Top: time series of NO, $NO_2$ and $O_3$ mixing ratios from a flight on July 21, 2004. Bottom: time series of measured (averaged to 30 s) and calculated (from Eq. (4)) $NO_3$, overlaid with the $j(NO_3)$ values (right axis).

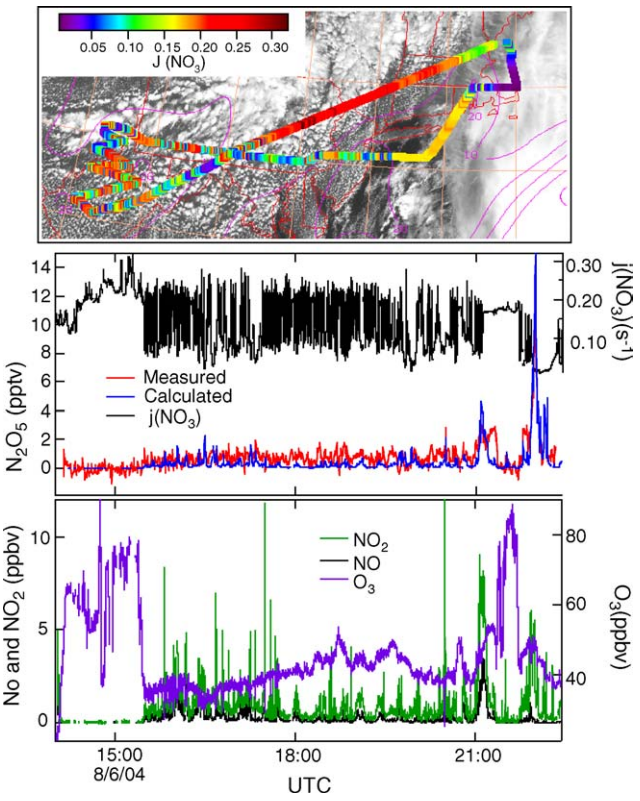


Fig. 2. Top: flight track from August 6, 2004, color coded according to the measured $j(NO_3)$ and overlaid on a satellite image of the cloud pattern for that day, illustrating the variation in $j(NO_3)$ observed as a result of clouds. Middle: time series of $j(NO_3)$, and measured (averaged to 5 s) and calculated (from Eq. (6)) $N_2O_5$. Fine variability in $j(NO_3)$ comes from the broken cloudiness over the Ohio River Valley. Bottom: time series of NO, $NO_2$ and $O_3$ mixing ratios.

and calculated $NO_3$ from a P-3 flight on July 21. The flight track on this day was mainly well to the east of New England over the Atlantic Ocean. Values of $j(NO_3)$ were consistently large, frequently in excess of 0.2 $s^{-1}$, possibly due to high albedo over low-level clouds. The small peaks in the observed $NO_3$ correspond with the steady-state predictions at 15:15 and 19:15 UTC. At these times there was enough $NO_2$ to generate a measurable amount of $NO_3$, but also, importantly, there was sufficient ozone (i.e., >100 ppbv) to drive the oxidation of $NO_2$, even in the case where $j(NO_3)$ was at its maximum, clear sky value.

Fig. 2 shows an example of the $N_2O_5$ observation from the time series on August 6, a day when the P-3 sampled power plant plumes in the Ohio River Valley over Pennsylvania, Ohio and West Virginia and then returned over the cities of New York and Boston. This example illustrates the widespread presence of $N_2O_5$ during the day in the presence of large $NO_x$ sources and/or persistent cloudiness that reduces the value of $j(NO_3)$. The top graph shows the flight track for this day, superimposed on a satellite image showing the cloud pattern. The power plants are evident from the spikes in the $NO_2$ time series in the lower graph in the middle of the flight, while the urban plumes appear as broader $NO_2$ peaks near the end of the flight. The fine-structure evident in the $j(NO_3)$ time series over the middle portion of the flight correlates with the broken cloudiness along the flight track over the upper Ohio River Valley. The clouds are expected to be at the top of the approximately 1.5 km planetary boundary layer, and the aircraft cruised at an altitude near 1 km in this region, underneath the broken clouds. Interestingly, there was a consistent, positive offset in the $N_2O_5$ signal throughout the region where $j(NO_3)$ was variable. This small signal was uncorrelated with the structure in the time series of the PAN compounds (sampled at 2 s resolution), which were present in small mixing ratios ($0.3 \pm 0.1$ ppbv for the sum of speciated PANs), although it is impossible to rule out a contribution from the PAN-correlated signal on the heated inlet to this signal. Other flights with similar levels of PAN but less variability in $j(NO_3)$ (e.g., the first leg of the July 15 flight described in the next section) exhibited no discernible $N_2O_5$ signal, although as noted above, the sensitivity to this signal was variable. Much of the structure that is discernible above the baseline noise in Fig. 2 correlates with the predictions of the daytime steady state calculated from Eq. (10), which is driven partly by structure in $NO_2$. Assuming it is not an artifact due to PAN, the generally positive offset of slightly less than 1 pptv in this region may be due to a similarity in the time scale required for the approach to steady state and the time scale on which these air masses are exposed to alternately larger and smaller $j(NO_3)$ due to the intermittent cloudiness. August 6 was a relatively cool summer day, with temperatures at the ~1 km cruising altitude of 12–13 °C. At this temperature, the approach to the daytime steady state for $N_2O_5$ requires roughly 10 min, sufficient to slow the response of the system under conditions of variable $j(NO_3)$ and degrade some of the predicted structure from the daytime steady-state calculation, which assumes essentially instantaneous response to changes in $NO_x$ or $j(NO_3)$.

Fig. 3 shows an expanded view of the latter portion of the August 6 flight, where the observed mixing ratio of $N_2O_5$ was well above the instrumental detection limit. Although this event occurred in the late afternoon, it was still 2–3 h prior to local sunset in this region. The increase in the observed $N_2O_5$ signal was due mainly to increased $NO_x$ in the region near New York city and Boston and a decrease in $j(NO_3)$ due to cloudiness at the point where the flight track crossed into the cloud deck off the New England coast. (Note that the satellite picture, taken at a single point in time, does not accurately reflect the particular clouds at any given point in the ~8 h flight, but it does give a general picture of the cloud pattern on that day.) The agreement between the predicted daytime steady state and the observed $N_2O_5$ is reasonable over most of this time period. The lower graph in Fig. 3 shows a correlation plot between the observed and calculated $N_2O_5$ mixing ratios. The only exception is the period just after 21:15, where the observation exceeds the prediction. Here, the observed signal correlated better with the measured PANs (which varied up to 1 ppbv) than with the predicted daytime $N_2O_5$ steady state. This example demonstrates that cloudiness can be a determining factor influencing $NO_3$ and $N_2O_5$ concentrations during the day. It also shows that the simple daytime steady-state expressions for $NO_3$ and $N_2O_5$ can reproduce the observed mixing ratios, and that the predicted steady-state concentrations of $NO_3$ and $N_2O_5$ can be used to assess their importance during daylight hours, even under conditions where their mixing ratios may be too small to observe definitively.

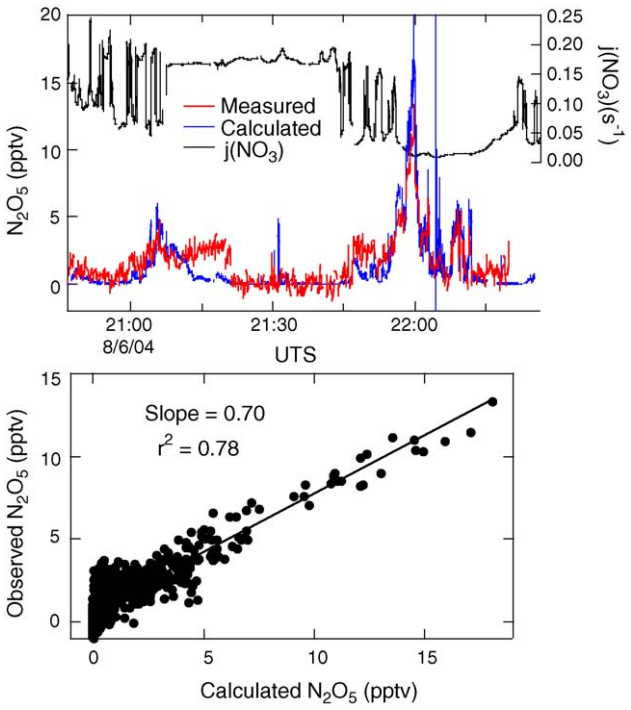


Fig. 3. Top: expanded view of the last two hours of the middle graph of Fig. 2. Bottom: plot of observed (averaged to 5 s) vs. calculated (according to Eq. (6)) $N_2O_5$ for the time period in the top graph. The correlation is good and the slope is 0.7, consistent with the $N_2O_5$ measurement being a lower limit, as discussed in the text.

## 5. Tropospheric implications

Although the observed and predicted concentrations of $NO_3$ and $N_2O_5$ are small in the presence of sunlight, they can still have an impact on tropospheric chemistry. As noted in the introduction, the production rate of $NO_3$ from the oxidation of $NO_2$ by $O_3$ is invariant with time of day, so that the flux through this oxidation process is always large. The primary reason for neglecting $NO_3$ during the day is that its photochemical destruction via channel (2a) leads to a null cycle.

$$NO_2 + O_3 \rightarrow NO_3 + O_2 \quad (1)$$

$$NO_3 + h\nu \rightarrow NO_2 + O \quad (2a)$$

$$O + O_2 \rightarrow O_3 \quad (11)$$

The sole result of this sequence is the absorption of photon of visible light. Furthermore, channel (2a) is the primary pathway for photolysis of $NO_3$, with a quantum yield, $\Phi(NO_2)$, of approximately 0.87 from atmospheric photolysis [20]. All other channels that effect some chemistry from the oxidation of $NO_2$ by $O_3$ during the day must compete with this rapid ($j \sim 0.2\,s^{-1}$) photolytic pathway. Nevertheless, there are several processes that can be of some importance under certain conditions. These include: (1) the perturbation of the Leighton photostationary state between NO and $NO_2$; (2) the photochemical destruction of $O_3$; (3) oxidation of reactive hydrocarbons; (4) conversion of $NO_x$ to nitric acid; (5) initiation of heterogeneous/multiphase chemistry from the uptake of $NO_3$ into droplets. Several of these topics have been discussed previously by Geyer et al. [7] in the context of daytime $NO_3$ observed at the surface under high $NO_x$ and $O_3$ conditions in Houston, TX. In this manuscript, we discuss the first four topics from the analysis of single events observed from the P-3 under conditions of generally lower $NO_x$ and $O_3$ away from the Earth's surface.

### 5.1. Perturbation of Leighton photostationary state

The only $NO_3$ destruction channel that is large in comparison to photolysis during the daytime is reaction of $NO_3$ with NO. The most important effect of this reaction is to modestly increase the oxidation rate of NO to $NO_2$ by $O_3$.

$$NO_2 + O_3 \rightarrow NO_3 + O_2 \quad (1)$$

$$NO_3 + NO \rightarrow 2NO_2 \quad (3)$$

$$\text{Net}: NO + O_3 \rightarrow NO_2 + O_2$$

One measure of the magnitude of the increased NO oxidation rate is the degree to which it perturbs the photostationary state between NO and $NO_2$ [25], described above (Eq. (7)). Geyer et al. [7] have given an expression for the Leighton ratio perturbed by the presence of $NO_3$.

$$\frac{[NO_2]}{[NO]} = \frac{k_8[O_3] + k_3[NO_3]_{Day}}{j_9} \quad (12)$$

For the majority of the daylight P-3 flights, the calculated Leighton perturbation due to $NO_3$ was quite small, of the order 0.5%. There were a number of brief periods of high $NO_x$ and/or low sunlight where it reached a maximum of 5%, although even a perturbation of this size would be difficult to discern in the NO and $NO_2$ data. By comparison, the predicted Leighton photostationary state perturbation due to the presence of peroxy radicals, which also convert NO to $NO_2$ (i.e., the key step in photochemical ozone production) can be on the order of 30% for $HO_2 + RO_2 = 100$ pptv [26]. Although the Leighton perturbation due to $NO_3$ for the 2004 P-3 data was largely insignificant, surface measurements in Houston, TX, have shown that it can be somewhat more important for low-light conditions near sunset [7].

### 5.2. Catalytic $O_3$ destruction

Photodissociation of $NO_3$ via its minor channel to give $NO + O_2$, with a quantum yield of $\Phi(NO) \approx 0.13$ for atmospheric photolysis [20], does not yield a null cycle but rather leads to catalytic ozone destruction.

$$NO + O_3 \rightarrow NO_2 + O_2 \quad (5)$$

$$NO_2 + O_3 \rightarrow NO_3 + O_2 \quad (1)$$

$$NO_3 + h\nu \rightarrow NO + O_2 \quad (2a)$$

$$\text{Net}: 2O_3 + h\nu \rightarrow 3O_2$$

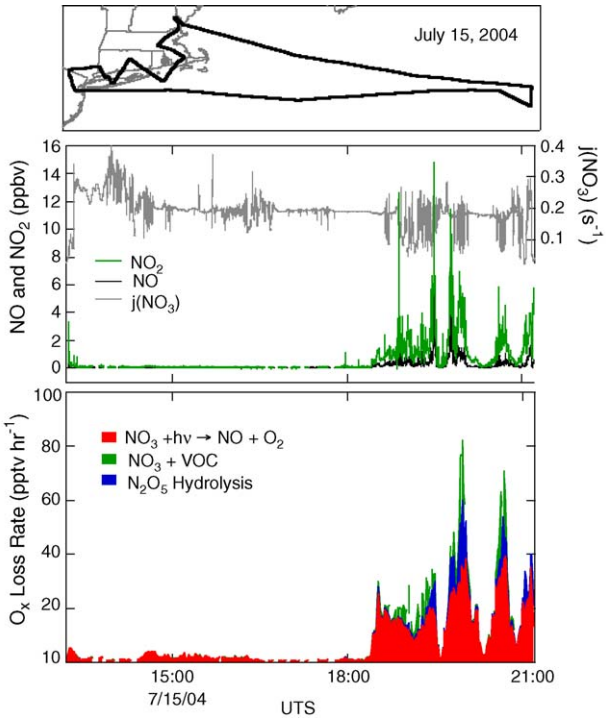


Fig. 4. Top: map showing the flight track for July 15, 2004. Middle: time series of NO and $NO_2$ mixing ratios and $j(NO_3)$ from this flight. Bottom: calculated $O_3$ loss rate due to the catalytic $O_3$ destruction cycle in Eq. (15) (red) summed with $O_x$ loss due to $N_2O_5$ hydrolysis (blue) and VOC oxidation (green).

The net loss rate for $O_3$ by this process is rate limited by reaction (1) times the fraction of the resulting $NO_3$ that is lost to the minor photolysis channel.

$$\frac{d[O_3]}{dt} = -2k_1[O_3][NO_2]\frac{\Phi(NO)\,j_2}{j_2 + k_3[NO]} \quad (13)$$

Here, the factor of 2 is due to the consumption of two $O_3$ for each $NO_3$ photolysis event. The calculated loss rates for $O_3$ by this channel are illustrated from the time series of the July 15 flight shown in Fig. 4. As shown by the map in the top graph, this flight initially sampled to the East, well out over the Atlantic Ocean, and then returned over New York city and Boston. The initial leg of this flight was characterized by relatively low $NO_x$ conditions, while the latter half sampled urban plumes. The $j(NO_3)$ was variable over the entire flight, but particularly so toward the end over the urban areas. This flight therefore contrasts the importance of daytime $NO_3$ and $N_2O_5$ chemistry under a variety of conditions. The lower figure shows three contributions to the odd oxygen, $O_x$, loss rate; the largest is the catalytic loss in Eq. (13). There are additional daytime losses of $O_x$ due to $NO_3$–VOC reactions and $N_2O_5$ hydrolysis that are also shown in this figure. These will be described in the following sections. Loss rates of $O_x$ due to $NO_3$ photolysis amounted to 10–50 pptv $h^{-1}$ on July 15, but only in the latter part of the flight where $NO_x$ was present and mainly in discrete $NO_x$ plumes. The largest daytime catalytic ozone loss rates calculated from the 2004 P-3 data set were roughly 100 pptv $h^{-1}$ within power plant plumes containing significant $NO_2$. Ozone loss rates of this order are small but non-negligible in comparison to other losses for ozone such as deposition, which can be estimated at ~500 pptv $h^{-1}$ in the daytime, continental boundary layer (e.g., deposition velocity of 0.4 cm $s^{-1}$ in a 1.5 km mixed layer [27]). For comparison, local production rates of ozone during the day can be on the order of several ppbv $h^{-1}$, and within urban plumes on the order of 10 ppbv $h^{-1}$ [26,28]. Thus, the catalytic loss of $O_3$ in the lower troposphere due to $NO_3$ photolysis may be on the order of 10% of the loss due to deposition, although it is likely 1% or less of the $NO_x$-driven production in VOC rich environments.

### 5.3. Daytime $NO_3$ oxidation of VOC

Oxidation of hydrocarbons during the day proceeds mainly by reaction with OH and $O_3$. Indeed, the small daytime concentrations of $NO_3$ discussed in this manuscript would make a negligible contribution to the oxidation of most hydrocarbons. However, $NO_3$ is highly reactive with unsaturated VOC in general and with certain biogenic compounds in particular [5,29]. Since even the small daytime $NO_3$ mixing ratios of ~0.5 pptv are comparable to peak OH concentrations, VOCs with rate coefficients for $NO_3$ oxidation that approach those of their OH reactions can be oxidized to a non-negligible extent during the day by $NO_3$. The two examples from the 2004 P-3 data that can be readily analyzed include isoprene and the monoterpenes. Both of these were measured with high time resolution and sensitivity by PTR-MS, although the monoterpenes include the sum of α- and β-pinenes and related compounds, all of which are quite reactive toward $NO_3$, $O_3$ and OH. For simplicity, monoterpenes will be treated as α-pinene, which is typically the largest observed component.

The oxidation rates for isoprene and monoterpenes in pptv $h^{-1}$ for isoprene and α-pinene from the flight on July 15 are shown in the lower two plots of Fig. 5. The loss rates are the products of the temperature-dependent rate coefficients for the reaction of the VOC with the oxidant, the oxidant concentration and the VOC mixing ratio.

$$\text{Loss rate (pptv h}^{-1}) = k_{\text{VOC+Oxidant}} \times [\text{Oxidant}] \times \text{VOC} \quad (14)$$

The concentrations of OH and $NO_3$ (shown in the upper plot) are calculated from a parameterization based on $NO_2$, $j(O_3)$ (to form O ($^1$D)) and $j(NO_2)$ [30], and from Eq. (4), respectively. The temperature-dependent rate coefficients are from the recent review of Atkinson and Arey [31]. The upper trace of the lower two plots is the ratio of the first-order loss rate coefficients for each VOC with respect to $NO_3$ to that for the sum of OH, $O_3$ and $NO_3$ (i.e., the ratios of the rate coefficients times the ratios of the oxidant concentrations, or the first two terms on the right-hand side of Eq. (14)), expressed as a percent. For isoprene, which has an OH reaction rate coefficient slightly more than 100 times that of $NO_3$ at room temperature, the oxidation due to the calculated $NO_3$ is never more than a few percent of the total. At the end of this flight, roughly two hours prior to local sunset, there were two time periods where the predicted $NO_3$-driven oxidation of isoprene was near 10% of the total. These events were the coincidence of $NO_x$ plumes with low $j(NO_3)$ and $j(O_3)$ under clouds. The upper trace shows that calculated

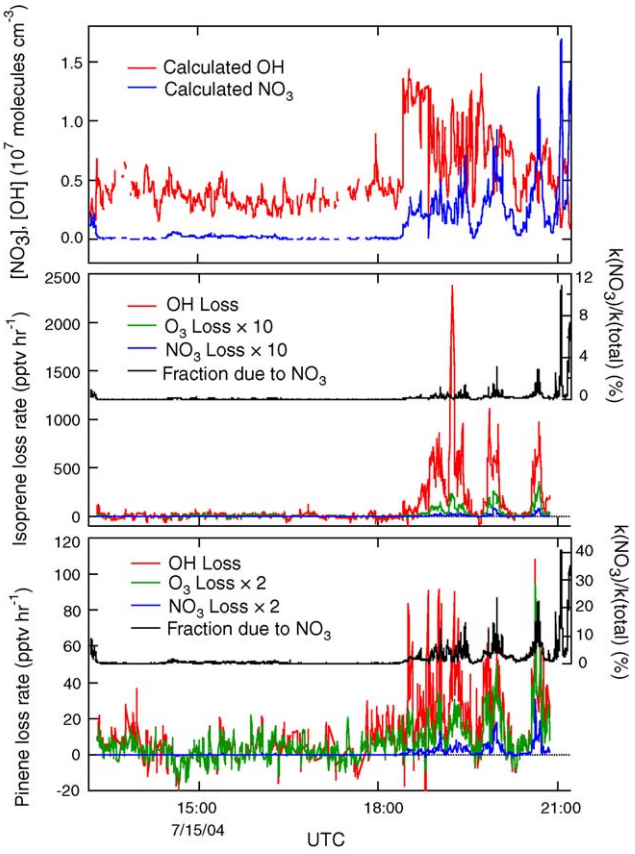


Fig. 5. Top: calculated concentrations for OH and $NO_3$ from the July 15 flight. Middle: calculated loss rates for isoprene due to OH, $O_3$ (×10) and $NO_3$ (×10) according to Eq. (14). Negative values are due to the scatter in the measured VOC mixing ratio about zero in regions of low mixing ratio. The right axis gives the ratio of the first-order loss rate coefficient for isoprene due to $NO_3$ oxidation to that for the sum of OH, $O_3$ and $NO_3$. Bottom: same as the middle plot, except for monoterpenes, with $O_3$ and $NO_3$ losses scaled by 2× rather than 10×, and with the rate coefficients taken as those for α-pinene.

$NO_3$ exceeded calculated OH by a factor of up to 17 under these conditions, the largest calculated daytime ratio of $NO_3$ to OH from the P-3 data. Unfortunately, neither the PTRMS VOC instrument nor the CaRDS $NO_3$ and $N_2O_5$ instrument was measuring at this time. One potential consequence of $NO_3$ oxidation of isoprene during the day would be the formation of oxidation products distinct from those due to OH or $O_3$. For example, OH reactions with isoprene lead largely to the formation of methyl vinyl ketone and methacrolein, whereas $NO_3$ oxidation leads to the formation of unsaturated organic nitrates [32].

Monoterpene oxidation by $NO_3$ is more important than isoprene oxidation because the ratios of the OH to the $NO_3$ rate coefficients are smaller (e.g., $k_{OH}/k_{NO_3} = 8.5$ for α-pinene at 298 K) [31]. The lower plot of Fig. 5 shows the importance of daylight monoterpene oxidation by $NO_3$ for the July 15 flight. Under the assumption that the oxidation rate coefficients for all monoterpenes are equal to that of α-pinene, the ratio of $NO_3$-driven oxidation to the total varied between 10 and 40%. In some cases, the first-order rate coefficient for $NO_3$ oxidation exceed that for OH. This result suggests that under cloudy conditions, monoterpene oxidation by $NO_3$ can be quite significant, and that even under clear sky conditions this oxidation can be non-negligible. For example, a calculation using the steady-state expressions given above shows that the fraction of the total α-pinene oxidation due to $NO_3$ (considering only gas phase reactions with OH, $O_3$ and $NO_3$) under clear sky conditions ($j(NO_3) = 0.2\ s^{-1}$) varies between 3 and 10% for 2 ppbv of $NO_2$ and $O_3$ in the range 50–150 ppbv. As Fig. 5 shows, this fraction increases considerably under low-light conditions. Such effects could be significant in environments such as forest canopies, where light levels are low but significant oxidation of very reactive biogenic hydrocarbons is known to occur [33,34].

These examples illustrate that $NO_x$-driven VOC oxidation via $NO_3$ formation can be an important loss pathway during the day for VOCs whose $NO_3$ reaction rate coefficients are within a factor of 100 times the OH rate coefficients. Other examples that are not analyzed here include certain aromatic compounds, such as phenols and styrenes, dimethyl sulfide (DMS), and oxidation products of biogenic compounds such as 3-methylfuran. It is important to stress the role of clouds in these oxidation processes. Because clouds can decrease both $j(NO_3)$ and $j(O_3)$ simultaneously, $NO_3$ oxidation under clouds will generally increase relative to OH. Furthermore, because late afternoon cloudiness is common in summer, when biogenic VOC emissions are important, $NO_3$ oxidation may play a larger role than previously considered in their oxidation. This result may have implications for $O_3$ formation in summer, which is driven by formation of peroxy radicals from oxidation of organic compounds in the presence of $NO_x$.

The preceding section noted that there can also be some ozone loss from the oxidation of VOC by $NO_3$. This is because each $NO_3$ contains two odd oxygen ($O_x$) (i.e., oxidation of NO to $NO_3$ requires two $O_3$). Therefore, loss of $NO_3$ to form, for example, organic nitrates in reactions with VOC effectively removes two $O_3$ for every $NO_3$ consumed. An upper limit to this odd oxygen loss can be estimated from the lower traces of Fig. 5 showing the VOC loss rates for $NO_3$. The corresponding ozone loss rates are equal to twice the total $NO_3$–VOC loss rates, assuming that the reaction leads to organic nitrates rather than to regeneration of $NO_2$ [35]. Summing both the isoprene and the monoterpene loss rates shown in the figure gives a net ozone loss in the presence of both $NO_x$ and VOC of several tens of pptv $h^{-1}$, and this loss has been added to the total $O_x$ loss calculation in Fig. 4.

### 5.4. Daytime hydrolysis of $N_2O_5$

The key step in the removal of $NO_x$ from the lower troposphere is the oxidation of $NO_2$ to $HNO_3$. During the day, this proceeds mainly by the reaction of OH with $NO_2$, whereas at night, one of the most important pathways is the heterogeneous hydrolysis of $N_2O_5$.

$$N_2O_5 + H_2O\,(\text{Het}) \rightarrow 2HNO_3 \qquad (15)$$

The daytime production rate of $HNO_3$ via this mechanism depends on the concentration of $N_2O_5$ and the first-order rate coefficient for reaction (15), which in turn depends on the available aerosol surface area density, $A$ ($\mu m^2\ cm^{-3}$), the uptake

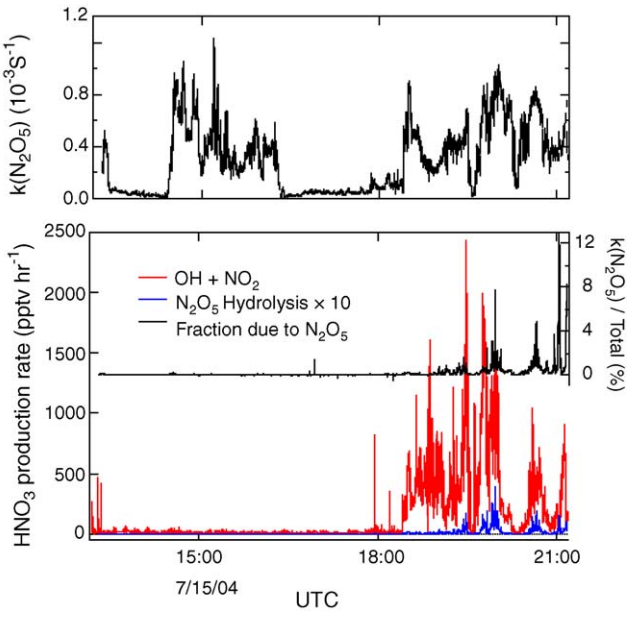


Fig. 6. Top: calculated first-order rate coefficient for $N_2O_5$ hydrolysis on aerosol surface, with $\gamma(N_2O_5) = 0.02$. Bottom: production rate for $HNO_3$ from both $OH + NO_2$ and from $N_2O_5$ hydrolysis. Overlaid against the right axis is the ratio of $HNO_3$ production from $N_2O_5$ hydrolysis to the total production.

coefficient for $N_2O_5$ on the aerosol surface, $\gamma(N_2O_5)$, and the mean molecular speed for $N_2O_5$, $c_{mean}$ [36].

$$\frac{d[HNO_3]}{dt} = 2k_{15}[N_2O_5]_{Day} \quad (16)$$

$$k_{15} \approx \frac{1}{4}\gamma(N_2O_5)c_{mean}A \quad (17)$$

Fig. 6 shows a comparison of the predicted rate of $HNO_3$ formation during the day from both $OH + NO_2$ and from $N_2O_5$ hydrolysis for the July 15 flight discussed in the preceding sections. Here, we have used calculated $N_2O_5$, the observed aerosol surface area density (corrected upward by 30% to account for the change in particle diameter between the relative humidity of the ambient air and that of the instrument [37]). The value for $\gamma(N_2O_5)$ is 0.02, based on laboratory measurements [38,39] and a recent determination from nocturnal aircraft measurements [40]. The corresponding lifetimes of $N_2O_5$ with respect to heterogeneous hydrolysis are on the order of 15–45 min and are shown as first-order loss rate coefficients in the top graph. The daytime $HNO_3$ production rates in Fig. 6 are estimates only because $\gamma(N_2O_5)$ has been taken as a constant; actual $\gamma(N_2O_5)$ in the atmosphere show considerable variability and may be larger or smaller than those shown here.

As in the analysis of VOC oxidation, the calculated $HNO_3$ production rate from daytime $N_2O_5$ hydrolysis is generally small in comparison to its photochemical analog from OH reactions, although there are certain situations in which it may be important. The ratio (as a percentage) of the $HNO_3$ production rate from $N_2O_5$ to the total is plotted against the right axis across the top of Fig. 6. Typical ratios within $NO_x$ plumes (the only place where $HNO_3$ production is significant) are on the order of a few percent, whereas ratios at the end of the flight under clouds are as large as 13%. It is important to note that the aerosol surface area densities were fairly modest, in the range from 150 to 600 $\mu m^2\,cm^{-3}$. Surface areas up to 2000 $\mu m^2\,cm^{-3}$ were observed during this campaign, and values consistently above 1000 $\mu m^2\,cm^{-3}$ have been seen in areas with large $SO_2$ emissions from coal-fired power plants. Therefore, enhancements in the conversion rate of $NO_2$ to $HNO_3$ due to $N_2O_5$ formation and hydrolysis in power plant plumes, where there is considerable $NO_x$ and sulfate aerosol from photochemical oxidation of $SO_2$, may be on the order of 5–10% under clear sky conditions and larger under cloudy conditions. This effect could be important in modeling the $O_3$ forming potential of such plumes, where the termination step in the $NO_x$ catalyzed formation of $O_3$ is the conversion of $NO_2$ to $HNO_3$.

As noted above, the conversion of $NO_x$ to $HNO_3$ via $N_2O_5$ also results in a modest loss of $O_3$ since the consumption of each $N_2O_5$ results in the loss of three $O_x$. Again, Fig. 4 shows this additional calculated $O_x$ loss term summed with the others due to $NO_3$ and $N_2O_5$ production. The two additional terms due to $NO_3$–VOC reactions and $N_2O_5$ hydrolysis nearly double that from $NO_3$ photolysis to $NO + O_2$ alone.

## 6. Conclusion

Small concentrations of $NO_3$ and $N_2O_5$ have been observed during the day from an aircraft platform using an in situ instrument. These are the first (to our knowledge) observations of $N_2O_5$ from a daytime source. A simple daytime steady-state expression reproduces the observations and allows some further predictions of their importance.

Reactions of $NO_3$ and $N_2O_5$ perturb the photostationary state between NO and $NO_2$, catalytically destroy ozone, and enhance the oxidation rate for biogenic VOC and the conversion of $NO_x$ to $HNO_3$. These effects are most significant under cloudy and/or high $NO_x$ conditions, where, for example, the contribution to oxidation of α-pinene by $NO_3$ or the production of $HNO_3$ from $N_2O_5$ hydrolysis may be approximately as important as their photochemical analogs from OH reactions. The daytime chemistry of $NO_3$ and $N_2O_5$ may also be of greater importance in other environments. The NEAQS-ITCT 2004 campaign took place during a summer that was characterized by low surface-level ozone concentrations. Since the $NO_3$ and $N_2O_5$ chemistry varies as the square of the ozone concentration under some conditions, particularly within urban plumes, it could make a larger contribution than observed here during high $O_3$ events in summer. In winter, on the other hand, when the thermal equilibrium between $NO_3$ and $N_2O_5$ shifts strongly in favor of the latter, effects such as $N_2O_5$ hydrolysis during the daytime could even dominate over $NO_2$ oxidation by OH. Furthermore, under cold conditions ($T < 260$ K, where the $N_2O_5$ lifetime exceeds 2 h [18]), $N_2O_5$ could have a long enough thermal lifetime during the day to be transported in this form and to provide a continuous source of daytime $NO_3$ and $NO_x$ from its thermal dissociation. Such effects could be important in lofted $NO_x$ plumes (e.g., from thunderstorm generated lightening $NO_x$) at the colder temperatures characteristic of the upper atmosphere. Daytime $NO_3$ chemistry in the marine boundary layer can be important to the oxidation

of DMS and to multiphase chemistry of $NO_3$ on fog droplets. Therefore, further tests of all of the effects of daytime $NO_3$ and $N_2O_5$ chemistry from the comparison of in situ measurements of $NO_3$ and $N_2O_5$ to their predicted, daytime levels in a variety of seasons and from different measurement platforms will be of considerable interest.

## Acknowledgements

ARR thanks Prof. Wayne for his scholarship and friendship over the years, and we all wish him the best in the future. This work was funded by NOAA's Climate Forcing Program of the Climate Goal and the Air Quality Program of the Weather and Water Goal.

## References

[1] R.P. Wayne, I. Barnes, P. Biggs, J.P. Burrows, C.E. Canosa-Mas, J. Hjorth, et al., Atmos. Environ. 25A (1991) 1–203.
[2] R.P. Wayne, Chemistry of Atmospheres, Oxford University Press, New York, 2000.
[3] J.F. Noxon, R.B. Norton, E. Marovich, Geophys. Res. Lett. 7 (1980) 125–128.
[4] U. Platt, D. Perner, A.M. Winer, G.W. Harris, J.N.J. Pitts, Geophys. Res. Lett. 7 (1980) 89–92.
[5] A.M. Winer, R. Atkinson, J.N.J. Pitts, Science 224 (1984) 156–158.
[6] U. Platt, F. Heintz, Isr. J. Chem. 34 (1994) 289–300.
[7] A. Geyer, B. Alicke, R. Ackermann, M. Martinez, H. Harder, W. Brune, et al., J. Geophys. Res. 108 (2003), doi:10.1029/2002JD002967.
[8] Y. Rudich, R.K. Talukdar, A.R. Ravishankara, J. Geophys. Res. 103 (1998) 16133–16143.
[9] G. Feingold, G.J. Frost, A.R. Ravishankara, J. Geophys. Res. 107 (2002), doi:10.1029/2002JD002288.
[10] P.A. Makar, F.J.D.D. Wang, R.M. Staebler, H.A. Wiebe, J. Geophys. Res. 104 (1999) 3581–3603.
[11] F.J. Dentener, P.J. Crutzen, J. Geophys. Res. 98 (1993) 7149–7163.
[12] T.B. Ryerson, E.J. Williams, F.C. Fehsenfeld, J. Geophys. Res. 105 (2000) 26447–26461.
[13] J.A. de Gouw, P.D. Goldan, C. Warneke, W.C. Kuster, J.M. Roberts, M. Marchewka, et al., J. Geophys. Res. 108 (2003), doi:10.1029/2003JD003863.
[14] C.A. Brock, M. Trainer, T.B. Ryerson, J.A. Neuman, D.D. Parrish, J.S. Holloway, et al., J. Geophys. Res. 108 (2003), doi:10.1029/2002JD002746.
[15] D.L. Slusher, L.G. Huey, D.J. Tanner, F. Flocke, J.M. Roberts, J. Geophys. Res. 109 (2004), doi:10.1029/2004JD004670.
[16] A. O'Keefe, D.A.G. Deacon, Rev. Sci. Instrum. 59 (1988) 2544–2551.
[17] R.A. Graham, H.S. Johnston, J. Phys. Chem. 82 (1978) 254–268.
[18] S.P. Sander, R.R. Friedl, D.M. Golden, M.J. Kurylo, R.E. Huie, V.L. Orkin, et al., Chemical Kinetics and Photochemical Data for Use in Atmospheric Studies, JPL Publication 02-25, Pasadena, CA, 2003.
[19] R.J. Yokelson, J.B. Burkholder, R.W. Fox, R.K. Talukdar, A.R. Ravishankara, J. Phys. Chem. 98 (1994) 13144–13150.
[20] H.S. Johnston, H.F. Davis, Y.T. Lee, J. Phys. Chem. 100 (1996) 4713–4723.
[21] F. Magnotta, H.S. Johnston, Geophys. Res. Lett. 7 (1980) 769–772.
[22] W.P. Dubé, S.S. Brown, H.D. Osthoff, S.J. Ciciora, M. Paris, R. McLaughlin, M.R. Nunley, A.R. Ravishankara, Rev. Sci. Instr., In preparation.
[23] S.S. Brown, H. Stark, S.J. Ciciora, R.J. McLaughlin, A.R. Ravishankara, Rev. Sci. Instrum. 73 (2002) 3291–3301.
[24] H.D. Osthoff, S.S. Brown, T.B. Ryerson, T.J. Fortin, B.M. Lerner, E.J. Williams, A. Pettersson, T. Baynard, W.P. Dube, S.J. Ciciora, A.R. Ravishankara, Anal. Chem., In preparation.
[25] P.A. Leighton, Photochemistry of Air Pollution, Academic Press, New York, 1961.
[26] G.J. Frost, M. Trainer, G. Allwine, M.P. Buhr, J.G. Calvert, C.A. Cantrell, et al., J. Geophys. Res. 103 (1998) 22491–22508.
[27] D.A. Hauglustaine, C. Granier, G.P. Brasseur, G. Megie, J. Geophys. Res. 99 (1994) 1173–1186.
[28] L.J. Nunnermacker, D. Imre, P.H. Daum, L. Kleinman, Y.N. Lee, J.H. Lee, et al., J. Geophys. Res. 103 (1998) 28129–28148.
[29] C. Warneke, J.A. de Gouw, P.D. Goldan, W.C. Kuster, E.J. Williams, B.M. Lerner, et al., J. Geophys. Res. 109 (2004), doi:10.1029/2003JD004424.
[30] D.H. Ehhalt, F. Rohrer, J. Geophys. Res. 105 (2000) 3565–3571.
[31] R. Atkinson, J. Arey, Chem. Rev. 103 (2003) 4605–4638.
[32] E.S.C. Kwok, S.M. Aschmann, J. Arey, R. Atkinson, Int. J. Chem. Kinet. 28 (1996) 925–934.
[33] A.H. Goldstein, M. McKay, M.R. Kurpius, G.W. Schade, A. Lee, R. Holzinger, et al., Geophys. Res. Lett. 21 (2004), doi:10.1029/2004GL021932.
[34] R. Holzinger, A. Lee, K.T. Paw, A.H. Goldstein, Atmos. Chem. Phys. 5 (2005) 67–75.
[35] I. Wangberg, I. Barnes, K.H. Becker, Environ. Sci. Technol. 31 (1997) 2130–2135.
[36] E.R. Lovejoy, D.R. Hanson, J. Phys. Chem. 99 (1995) 2080–2087.
[37] M.Y. Choi, C.K. Chan, Environ. Sci. Technol. 36 (2002) 2422–2428.
[38] M. Hallquist, D.J. Stewart, S.K. Stephenson, R.A. Cox, Phys. Chem. Chem. Phys. 5 (2003) 3453–3463.
[39] S.M. Kane, F. Caloz, M.-T. Leu, J. Phys. Chem. A 105 (2001) 6465–6470.
[40] S.S. Brown, T.B. Ryerson, A.G. Wollny, C.A. Brock, R. Peltier, A.P. Sullivan, et al., In preparation.